# Supporting Information

## A Carbonyl Decorated Two-Dimensional Polymer as a Charge-Trapping Layer for Non-Volatile Memory Storage Device with a High Endurance and a Wide Memory Window

*Ruba Al-Ajeil, [#] Abdul Khayum Mohammed, [#] Pratibha Pal, [#] Matthew A. Addicoat, Surabhi Suresh Nair, Dayanand Kumar, Abdul Momin Syed, Ayman Rezk, Nirpendra Singh, Ammar Nayfeh, Nazek El-Atab,* Dinesh Shetty**

### General remarks

All chemicals and solvents were commercially purchased and used without further purification. *1, 3, 5*-triformylphloroglucinol was purchased from 'Hygeia laboratories'. *1, 4*-diacetylbenzene (Db) and p-toluene sulfonic acid (PTSA) were purchased from TCI.

### Instruments

***FT-IR***: Fourier transform infrared (FT-IR) spectra were obtained using a Bruker Optics ALPHA-E spectrometer with a universal Zn-Se ATR (attenuated total reflection) accessory or using a Diamond ATR (Golden Gate) in the 600-4000 $cm^{-1}$ region.

***Thermogravimetric analyses (TGA)***:TGA was carried out on a PerkinElmer Simultaneous ThermalanalyzerSTA 6000 under $N_2$ atmosphere.

***Scanning Electron Microscopy (SEM)***:The JEOL JSM-7610F FEG-SEM and Helios SEM were used for the SEM analysis of TpDb. It combines an electron column with semi-in-lens detectors and an in-the-lens Schottky field emission gun to deliver ultrahigh-resolution with a wide range of probe currents (1pA to more than 200 nA).

***Solid-state UV-visible spectra***: The solid-state UV-visible spectral analysis was carried out using The LAMBDA 1050 UV/Vis/NIR spectrometer.

***Powder X-ray Diffraction Data of Fe-Tp***: For the crystallinity analysis, Bruker D2 Phaser XRD, X-ray source with CuKα radiation. Data was collected in the 2θ range from 5° to 50°, with step size 0.05° and 0.5 s / step.

**Synthesis of TpDb**

TpDb was synthesized through a mechanomixing solid-state synthetic strategy. *1, 4*-diacetylbenzene (Db) was added along with the p-toluene sulfonic acid (PTSA) catalyst in a ratio of (1:5) and grinded manually for a period of time at room temperature to initiate the enol formation. Then *1, 3, 5*-Triformylphloroglucinol (Tp) was added to the Db + PTSA mixture (keeping the mole ratio of *1: 1.5* (Tp: Db)) and ground until the formation of homogeneous mixture. The obtained final mixture (a white paste) was kept in the oven at 90 °C for 24 hours. The black-colored sample was washed with water; N, N-dimethylacetamide (DMA), and acetone.

Furthermore, the thin sheet of TpDb was fabricated by casting the final white-colored paste (Tp + Db + PTSA) directly on a glass surface. It was further heated in a closed environment at 90 °C for 24 hours. Notably, the colour of the white paste was abruptly changed to black within a few minutes (Figure S2).

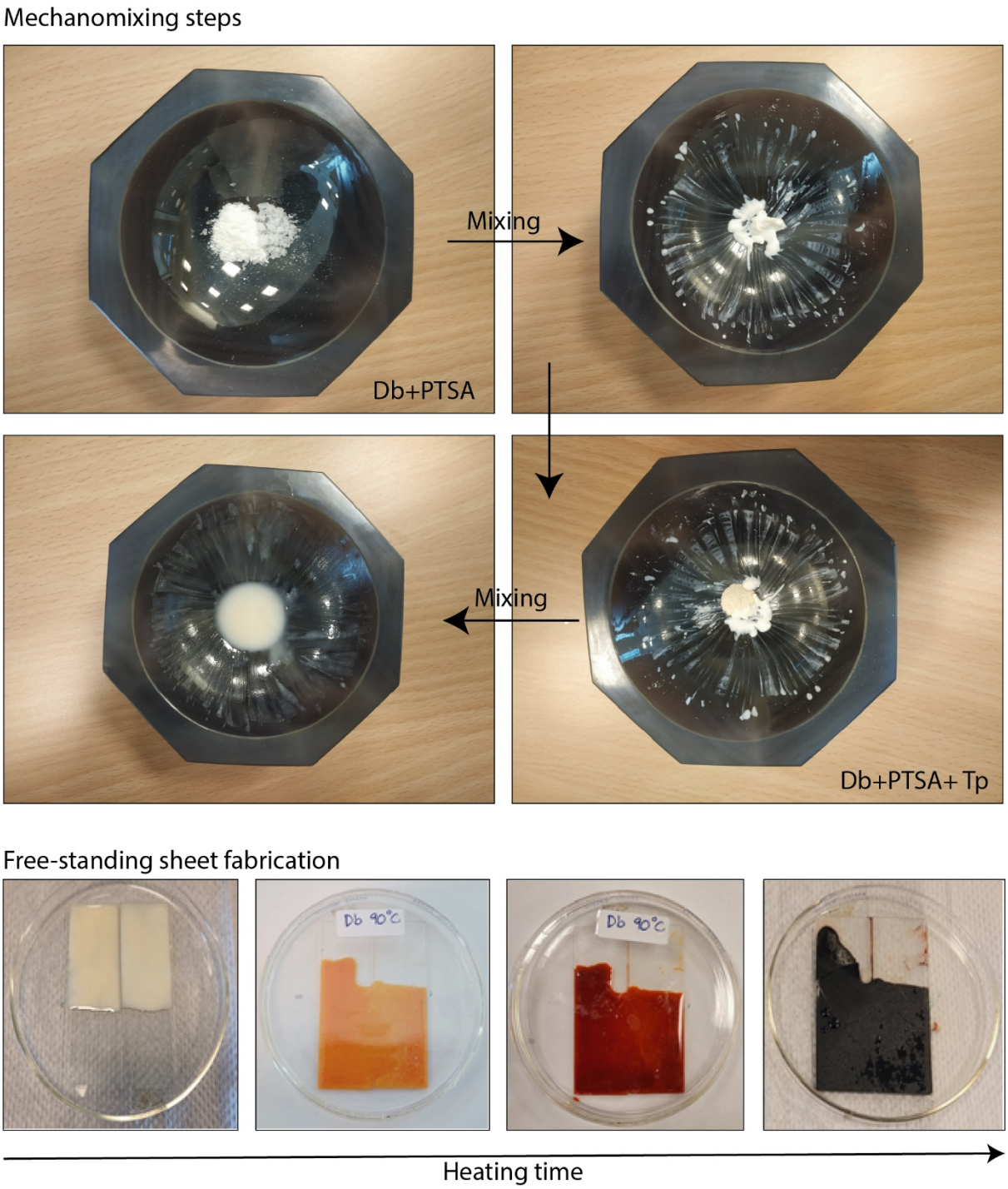


**Figure S1**: The digital photograph of mechanochemical synthesis of TpDb and Tp-Db thin sheet imaged every 15 minutes at 90 ºC.

**SEM of TpDb**

Scanning electron microscopy of TpDb obtained using Quanta 250 FEG SEM. The material was coated with platinum and positioned vertically for the cross sectional analysis and horizontally for planar imaging. The surface morphology of TpDb was slightly brittle and

showed minor cracks however, it is still considered a free-standing thin sheet and showed a fairly uniform surface signifying homogeneity. The average cross-sectional thicknesses of the thin sheets were obtained for comparative electrical conductivity studies. The fabrication technique resulted in thin sheet thicknesses that were at their thinnest in the micrometer range.

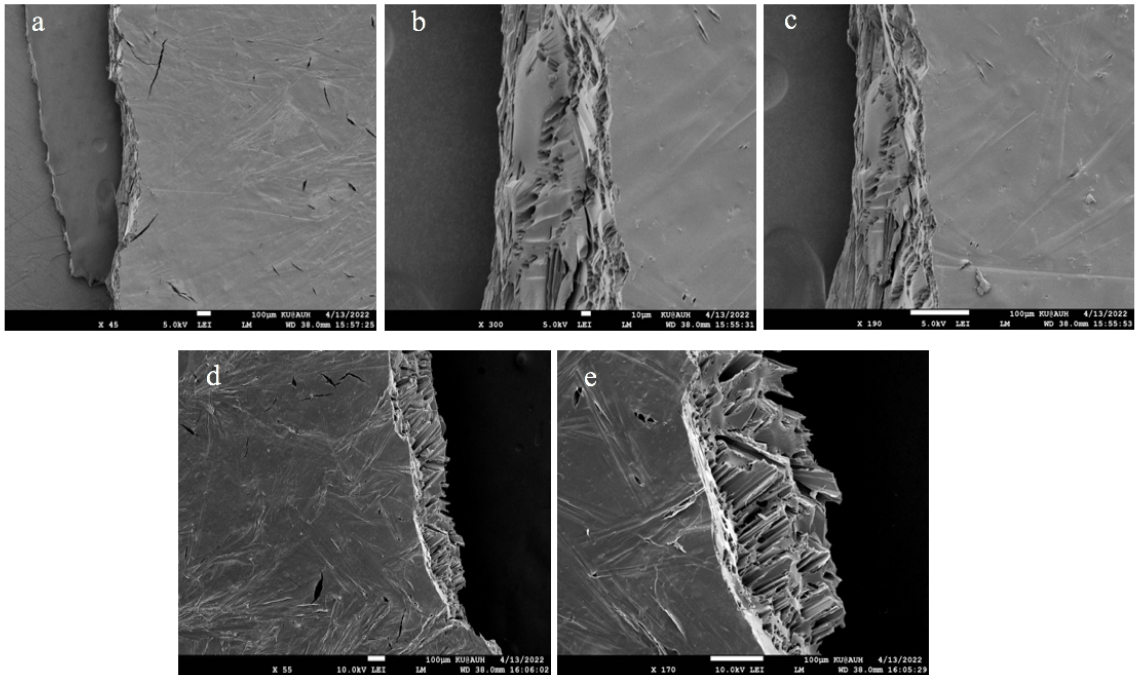


**Figure S2**: SEM images of TpDb monoliths (herein free-standing sheets).

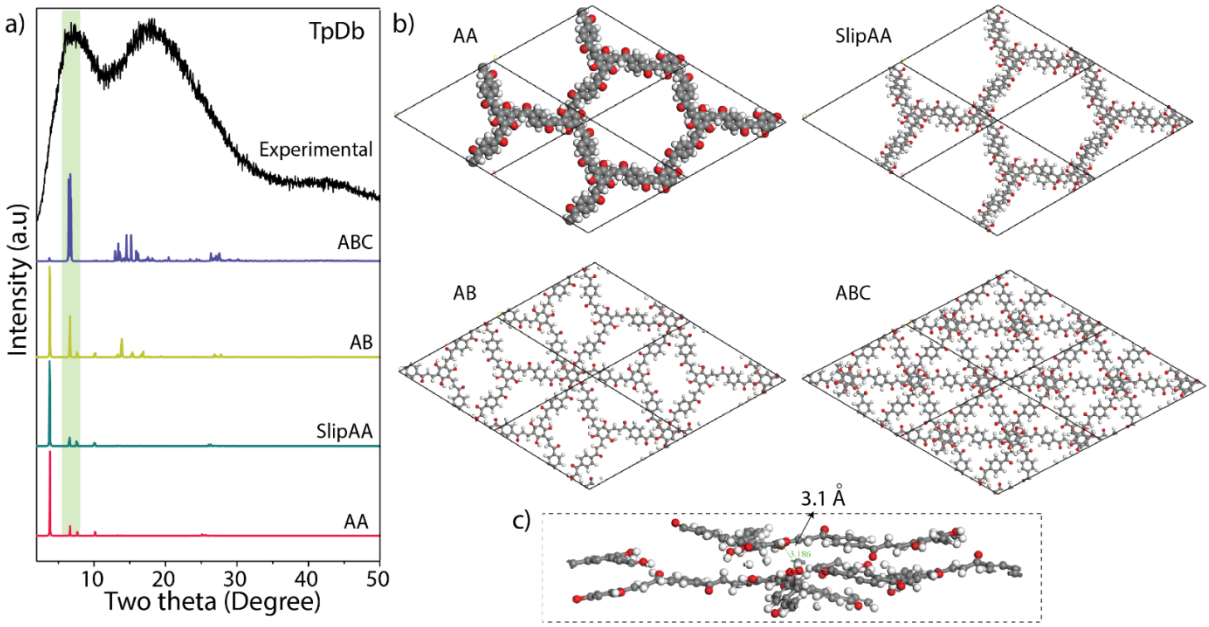


**Figure S3**: The experimental PXRD profile of TpDb with simulated PXRD of various stacking possibilities; b) The theoretical models of various stacking

models (2 x 2 cells); and c) The possible interlayer interaction through hydrogen bonding (3.1 Å) in the ABC stacking.

Atomic positions and cell sizes of the TpDb was optimized using the Self Consistent-Charge Density Functional Tight-Binding (SCC DFTB) method, including LennardJones dispersion. C, N, O, H atoms were described using the mio-0-1 parameter set (*M. Elstner et al., Phys. Rev. B, 1998, 58, 7260*).

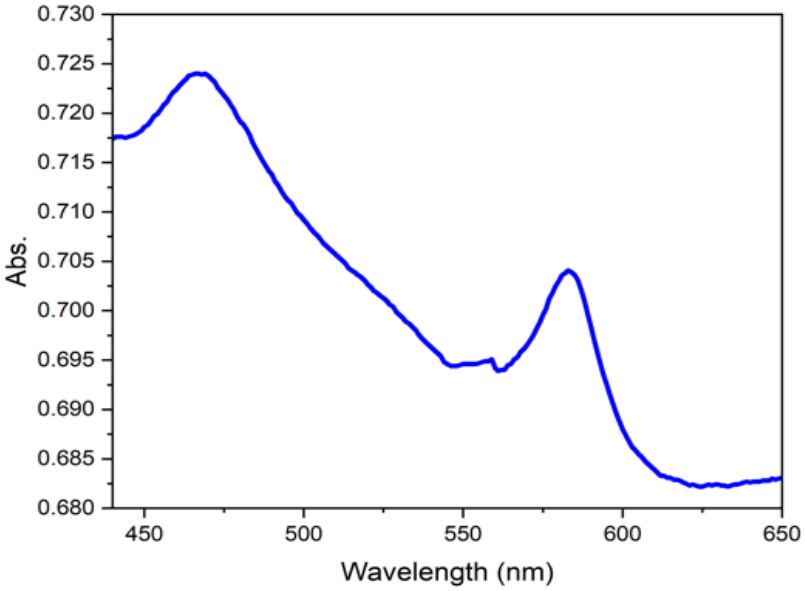


**Figure S4**: The solid-state UV-visible spectrum of TpDb.

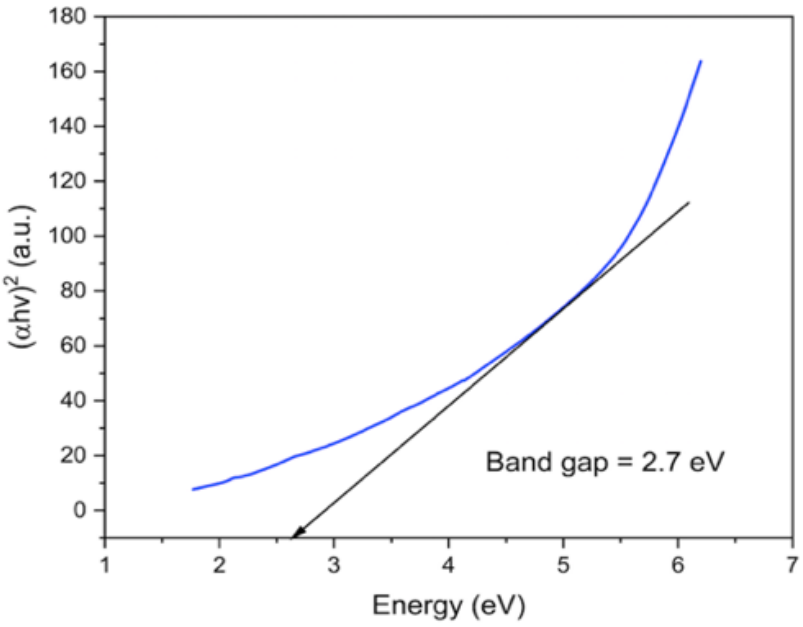


**Figure S5**: The Tauc plot of TpDb.

**Electrical conductivity measurements of TpDb**

The electrical conductivity measurements of the free-standing sheets were analyzed by a four-probe method. The Signatone four-probe instrument was employed to measure the bulk conductivity of TpDb thin sheets by supplying a known voltage whereby the current that passes through it was measured to obtain the resistance through Ohm's law. Each of the four probes was equally spaced from each other at approximately 0.75 cm in which the outer two wires were used to provide a known amount of current and the inner ones calculated the potential drop that resulted from the applied current. A linear current-voltage (I-V) profile was obtained that is indicative of ohmic conduction. The slopes of the graphs yielded conductance and the reciprocal of the slope resulted in the conductivity value of $5.83*10^{-9}$ S $m^{-1}$ and $6.32*10^{-9}$ S $m^{-1}$ respectively as shown in Figure S8. For the experimental setup, the samples were cut carefully using scissors to obtain dimensions of approximately 2 x 2 $cm^2$ as a laser cutter would be impossible to accommodate owing to their brittle nature. The bulk electrical conductivity was then measured with the gold-plated probes equally spaced and placed with appropriate distance from the edge to avoid edge effect.

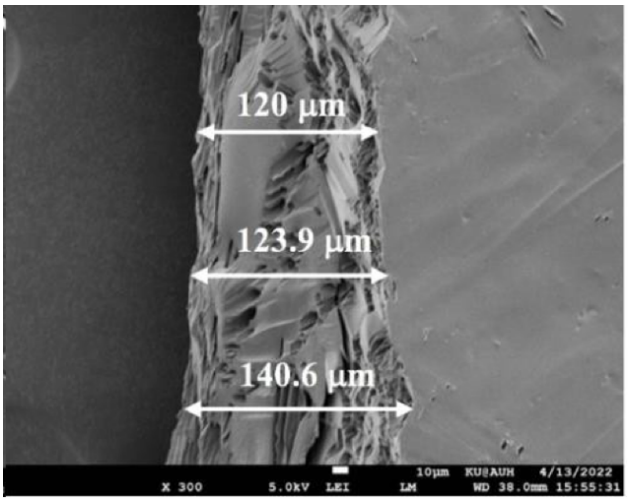


**Figure S6**: SEM of TpDb thin sheet with thickness.

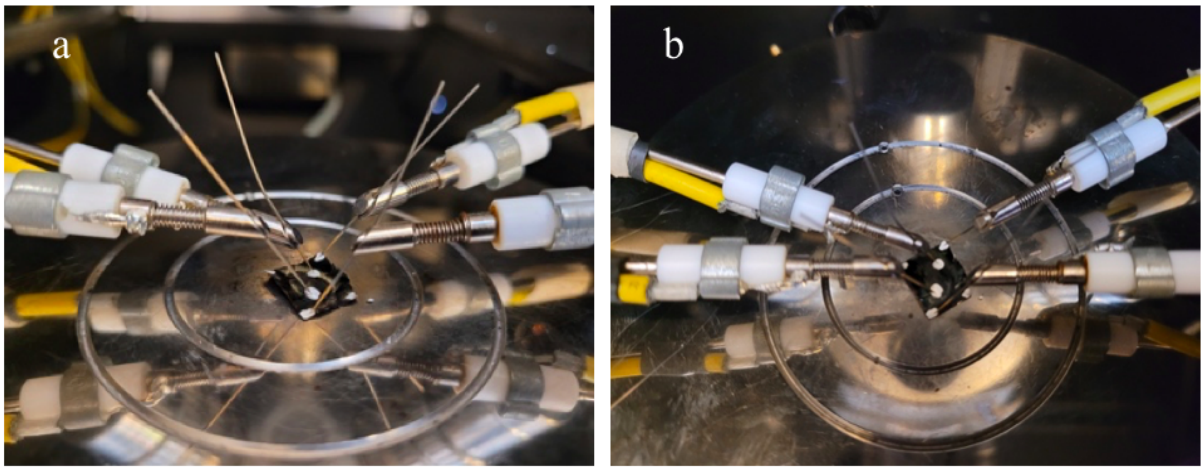


**Figure S7**: Experimental set-up of TpDb thin sheet in Signatone Probe Station (a) in plane and (b) out of plane

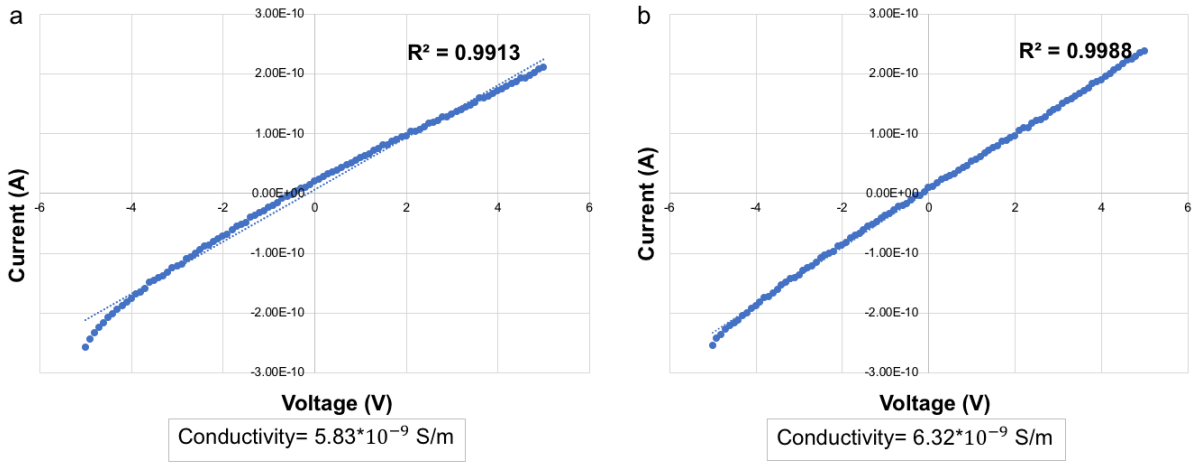


**Figure S8**: Electrical conductivity measurements of TpDb thin sheets with thickness (a) 128 µm, and (b) 200 µm.

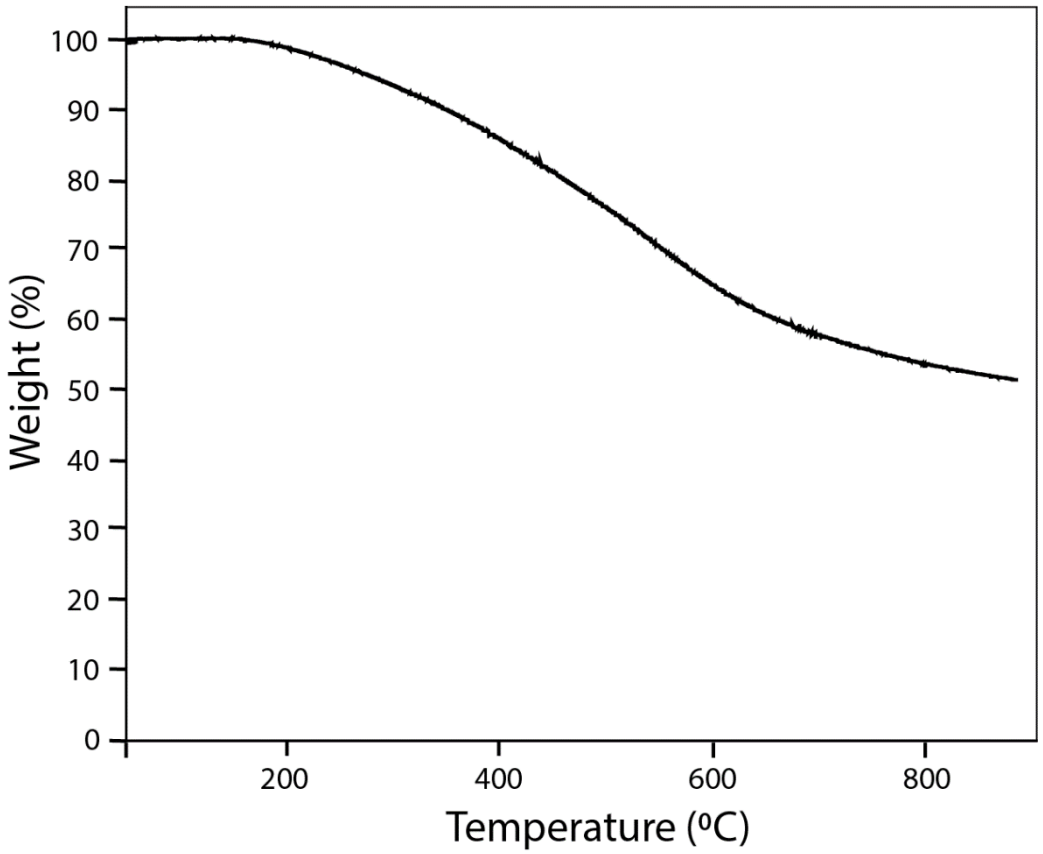


**Figure S9**: TGA of TpDb. It shows a thermal stability up to 200 °C.

**Computational details**

Density functional theory calculations for the ABC-stacked model of TpDb were conducted using the projector-augmented wave method as implemented in the Vienna Ab initio Simulation Package (VASP),[1] employing the Perdew–Burke–Ernzerhof functional within the generalized gradient approximation scheme.[2] Ionic relaxation of the ABC-stacked TpDb model was rigorously executed at the gamma point until Hellmann–Feynman forces subsided below $10^{-3}$ eV/Å and total energy descended to levels below $10^{-6}$ eV. Self-consistent calculations were performed with precision, utilizing a kinetic energy cutoff of 500 eV for the plane wave basis set and employing a 1 × 1 × 1 k-mesh.

The electron affinity, a key metric in this investigation, was calculated as the discerning energy distinction between the vacuum level ($E_{vac}$) and the conduction band minimum ($E_C$),[3]

$E_{ea} = E_{vac} - E_c$

**Preparation of TpDb solution**

Figure S10 shows a schematic diagram of the preparation of TpDb solution. Bulk TpDb sample was mechanically grounded by using mortar and pestle [4] . Before, hand milling, 2-3 drops of methanol were added at room temperature. Then milling was performed for 30 minutes. The crushed fine particles were collected and dispersed in isopropanol (IPA). Then the solution was stirred at 500 rpm for 15 hours. The obtained solution was said as TpDb solution, which was further used for drop-casting on Al 2 O 3 layer to aim charge-trapping memory device fabrication.

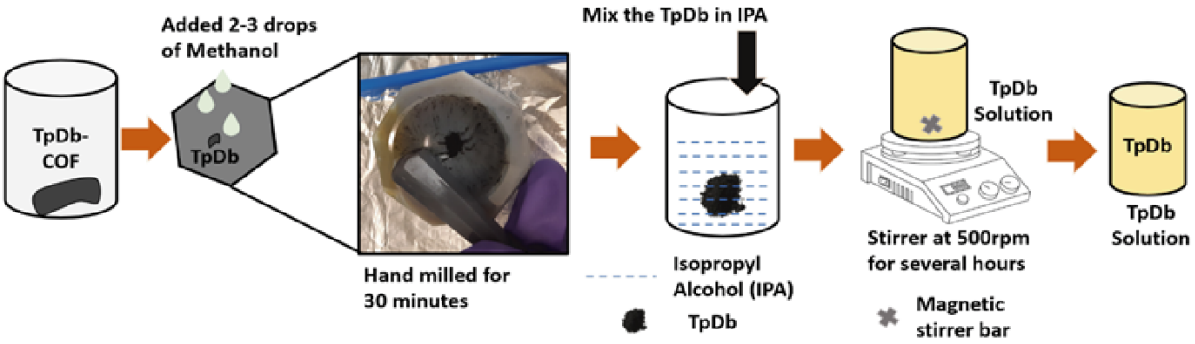


**Figure S10**: Schematic diagram of the preparation of TpDb solution for drop casting.

**Fabrication process flow of MOS capacitor Al/$Al_2O_3$/TpDb/$Al_2O_3$/Si device**

Figure S11 shows a schematic diagram of the fabrication process flow.

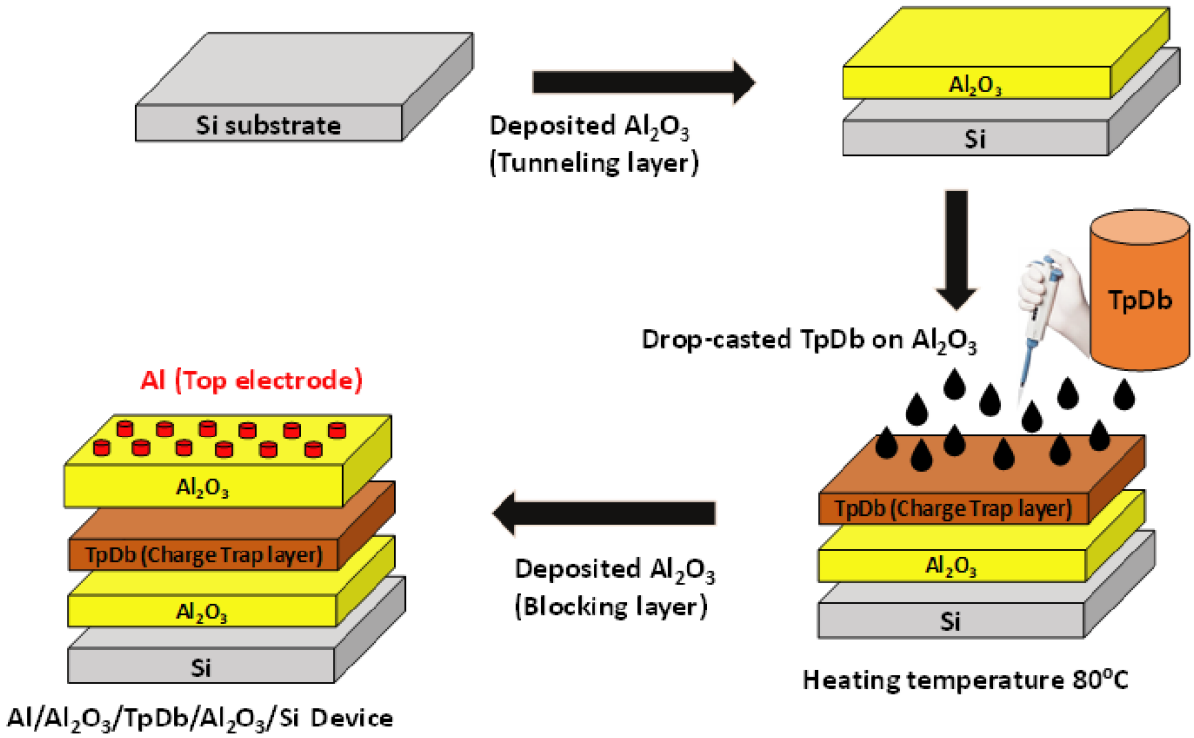


**Figure S11**: Schematic diagram of the fabrication process flow of Al/$Al_2O_3$/TpDb/$Al_2O_3$/Si CTM device.

**Structural and electrical characterization of the MOS capacitor**

To examine the surface morphology of TpDb, scanning electron microscopy (SEM) was carried out using Megellan-SEM device operated at an accelerating voltage 3 kV. Before the SEM examination, the sample were sputter-coated with a 3 nm thickness of iridium layer. All the electrical characterizations were carried out using a Keysight B1500 A semiconductor device probe station.

**Breakdown voltage measurement and Electric field intensity calculation**

Including the breakdown voltage and electric field intensity is an important parameter for characterizing CTM. The break down voltage $V_{br}$ was found to be around 12V, as shown in Figure S12.

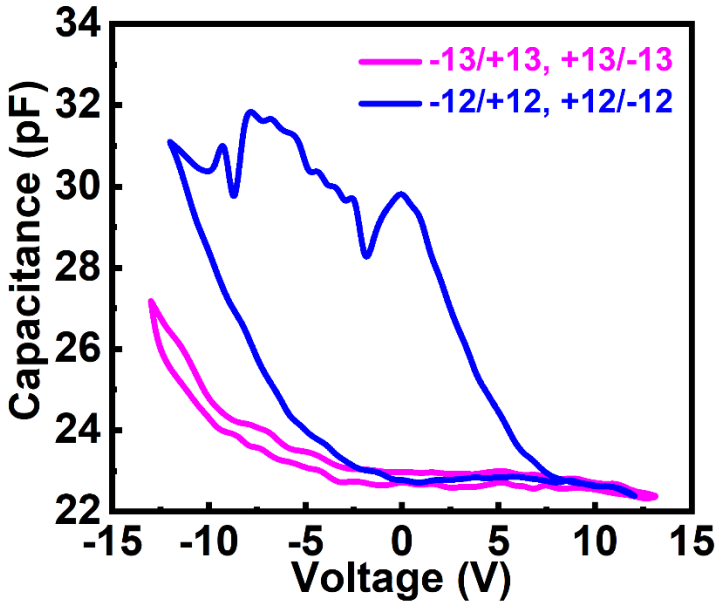


**Figure S12**: Breakdown voltage of the Al/$Al_2O_3$/TpDb/$Al_2O_3$/Si MOS capacitor.

We also calculated the electric field intensity induced across the tunnel oxide and charge trapping layer, using an estimation for the dielectric constant of the TpDb. Assuming that the change in the threshold voltage ($^{\Delta V_{th}}$) is primarily due to the charges stored in the TpDb layer, we can estimate the charge trap states density (*N)* using the following equation:

$N = \frac{C.\Delta V_{th}}{q}$ where the capacitance per unit area ($C$) is given by $C = \frac{\varepsilon_0.\varepsilon_{Al_2O_3}.\varepsilon_{TpDb}}{\varepsilon_{TpDb}.t_{Al_2O_3} + \varepsilon_{Al_2O_3}.t_{TpDb}}$

Where $\varepsilon_0$, $^{\varepsilon_{Al_2O_3}}$, and $\varepsilon_{TpDb}$ are the dielectric constant of free space, $Al_2O_3$ and TpDb, respectively. $^{t_{Al_2O_3}}$and $t_{TpDb}$ are the thicknesses of $Al_2O_3$ and TpDb layers, respectively. $^{\Delta V_{th}}$ is the change in threshold voltage of the on-and-off states of the memory at breakdown voltage $V_{br}$ and q is the elementary charge.

The resulting electric field across the TO can be calculated as [5] :

$$E_1 = \frac{V_{br}}{t_1 + t_2.\left(\frac{\varepsilon_1}{\varepsilon_2}\right) + t_3.\left(\frac{\varepsilon_1}{\varepsilon_3}\right)} + \frac{q.N}{\varepsilon_0.(\varepsilon_1 + \varepsilon_2.\left(\frac{t_1}{t_2}\right) + \epsilon_3.\left(\frac{t_1}{t_3}\right))}$$

Here, $\varepsilon$ is the dielectric permittivity, t is the layer thickness, and the subscripts 1, 2, and 3 correspond to the TO, BO, and TpDb, respectively.

| $\varepsilon_{TpDb}$ | **1** | **2** | **3** | **4** | **5** | |
|---|---|---|---|---|---|---|
| $C$ | 1.43 | 2.77 | 4.02 | 5.21 | 6.32 | F/cm$^2$ |
| $N$ | 8.91×10$^{11}$ | 1.73×10$^{12}$ | 2.51×10$^{12}$ | 3.25×10$^{12}$ | 3.95×10$^{12}$ | cm$^{-2}$ |
| $E_{TO}$ | 0.36 | 0.70 | 1.02 | 1.32 | 1.60 | MV/cm |

| | | | | | | |
|---|---|---|---|---|---|---|
| $E_{TpDb}$ | 1.94 | 1.89 | 1.84 | 1.79 | 1.75 | MV/cm |

The calculated breakdown electric field intensity (E) ranged between 0.36 and 1.6 MV/cm across the TO layer and between 1.94 and 1.75 MV/cm across the TpDb layer, assuming ε_TpDb falls within 1 to 5 [6]. It should be noted that the breakdown electric field of Al2O3 is generally above 10 MV/cm [7]. Thus, we expect the memory to be breaking down due to the polymer break down.

**Frequency dependent capacitance characteristics of the device**

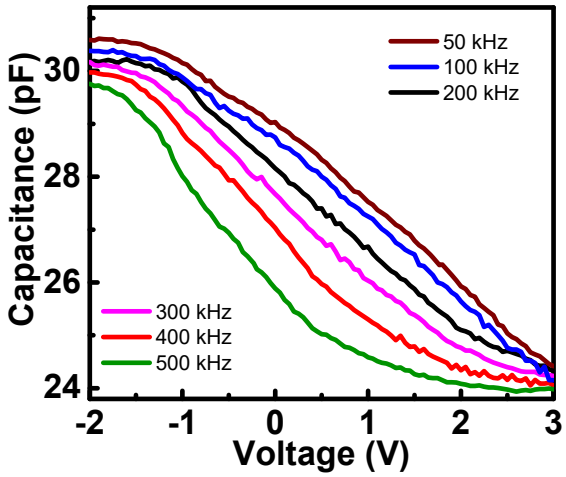


**Figure S13**: Frequency dependent capacitance characteristics. The frequency hysteresis confirms the presence of interfacial trap states at $Al_2O_3$/TpDb interface.

**I-V characteristics of the device**

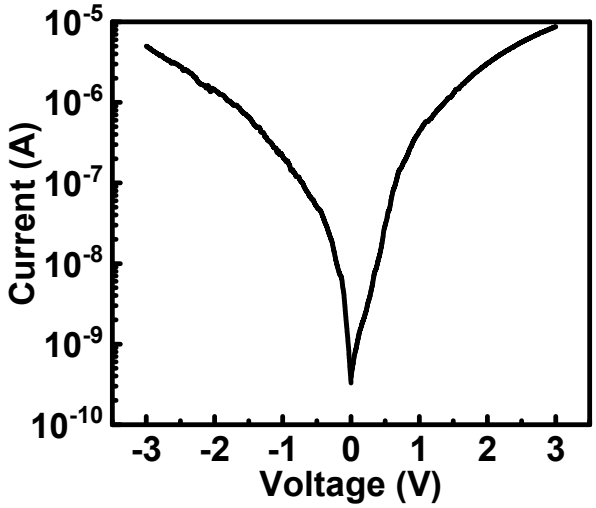

**Figure S14**: I-V characteristics of the device.

**Comparison of previously reported charge trapping materials with this work**

**Table S1:** Comparison between the previously reported memory performance based on different charge trapping materials and the demonstrated $Al/Al_2O_3/TpDb/Al_2O_3/Si$ device in this work.

| Sl. No | Charge Trapping layer | Device structure | Sweeping Voltage | Charge Density ($cm^{-2}$) | Memory Window | Endurance | Retention | Application | Ref |
|---|---|---|---|---|---|---|---|---|---|
| 1 | ***TpDb*** | ***$Al/Al_2O_3/TpDb/Al_2O_3/Si$*** | ***(-8 V/+8 V)*** | ***$1.562 \times 10^{13}$*** | ***3.2 V*** | ***10000 cycles*** | ***$10^4$ s*** | ***Non-volatile memory*** | *This work* |
| 2 | Dodecanethiol Nanoparticle-based polymer memory devices (PMDs) | Al/PVP/dodecanethiol nanoparticles/$SiO_2$/Si | (-6 V/+6 V) | $3.3\times10^{12}$ | 1.8 V | NA | 6 H | Dodecanethiol Nanoparticle-based polymer memory devices (PMDs) | 8 |
| 3 | Pentacene and tris(8-hydroxyquinoline) aluminum (Alq3) | Au/Pentacene and $Alq_3/SiO_2$/Si | (-80 V/+80 V) | NA | ~40 V | 100 cycles | $10^3$ s | Organic non-volatile memory applications | 9 |
| 4 | Naphthalene diimide-alt-biselenophene) (PNDIBS) | Ag/PNDIBS/$SiO_2$/Si | (-60 V/+60 V) | NA | 28 V | 200 cycles | 800 s | OFET memory devices | 10 |
| 5 | Poly(allyl amine) (PAH)/poly(styrene sulphonate) (PSS) (PAH/PSS/PAH/AuNP)n=1-4 | [Pt/HfOx/CTM/HfOx/Si] | (-8 V/+20 V) | $4.2 \times 10^{12}$ | 1.8 V | NA | 7 days | Non-volatile memory | 11 |
| 6 | Self-assembled PS-b-P4VP with Au nanoparti | Au/Pentacene/PS-b-P4VP/$SiO_2$/Si | (-10 V/+10 V) | $9.07 \times 10^{10}$ | 1 V | NA | $6\times10^4$ s | Non-volatile memory | 12 |

| | | | | | | | | | |
|---|---|---|---|---|---|---|---|---|---|
| | cles | | | | | | | | |
| 7 | Pentacene | Au/Pentacene/$Al_2O_3$/ITO/PET film (APTES device) | (-50V/+50 V) | $9 \times 10^{10}$ | 16.5 V | >1000 cycles | $10^5$ s | Flash memories | 13 |
| 8 | GaAs MOS Capacitor With Polymer-Based Thin Film | Au/Ni/SICON polymer based film/GaAs/Pt/Ti/Pt/Au | (-4 V/+4 V) | 9.7 x $10^9$ | 0.5 V | NA | NA | NA | 14 |
| 9 | ZnO nanodisc arrays | Au/$SiO_2$/ZnOnanodisc/$SiO_2$/Si/Pt | (-10 V/+5 V) | 2.3 × $10^{18}$ | 1.9 V | NA | $10^3$ s | Dye-sensitized solar cells and Charge coupled devices (CCDs) | 15 |
| 10 | Polyelectrolytes | Al/Cobalt bionanodot-accommodated ferritin /polyelectrolyte/$SiO_2$/Si | (−7 V/+5 V) | NA | 1.9 V | NA | NA | Non-volatile memory | 16 |
| 11 | Acetylene-linked Pyrene-Isoindigo (PI) 2D-CMP NPs | $Al_2O_3$/PI-NPs/$Al_2O_3$/Ge | (-4 V/+4 V) | 3 × $10^6$ | 1.5 V | 1000 cycles | $10^4$ s | NA | 17 |

## References


[1] G. Kresse, J. Furthmüller, Phys Rev B Condens Matter Mater Phys 1996, 54, 11169–11186.

[2] S. Grimme, J. Antony, S. Ehrlich, H. Krieg, Journal of Chemical Physics 2010, 132, DOI 10.1063/1.3382344.

[3] Z. Zhang, M. Wensell, J. Bernholc, Phys Rev B 1995, 51, 5291–5296.

[4] C. Wang, Z. Zhang, Y. Zhu, C. Yang, J. Wu, W. Hu, Adv. Mater. 2022, 34, 2102290. https://doi.org/10.1002/adma.202102290.

[5] S.M. Sze, Kwok K. Ng, Physics of Semiconductor Devices, third ed., Ch. 6, Pg. 353, John Wiley & Sons, JNC, Hokoben, New Jersey, (2007).

[6] Boosting exciton dissociation by regulating dielectric constant in covalent organic framework for photocatalysis, Guoqing Li et al., Chem Catalysis, Volume 2, Issue 7, 1734 – 1747, DOI: 10.1016/j.checat.2022.05.002.

[7] Lin, H.C., Ye, P.D. and Wilk, G.D. (2005) 'Leakage current and breakdown electric-field studies on Ultrathin Atomic-layer-deposited al2o3 on GaAs', Applied Physics Letters, 87(18). DOI:10.1063/1.2120904.

[8] D. Prime, S. Paul and P. W. Josephs-Franks, Philosophical Transactions of the Royal Society A: Mathematical, Physical and Engineering Sciences , 2009, vol. 367, no. 1905, doi: 10.1098/rsta.2009.0141.

[9] J-H Hong, S. H. Kim, S. B. Jo, K. Cho, B. Kang, Organic Electronics, 2011, Volume 93, 106107.
[10] N. M. Murari, Y.-J. Hwang, F. S. Kim, S. A. Jenekhe, Organic Electronics 2016, Volume 31, Pages 104-110.
[11] J.-S. Lee, J. Cho, C. Lee, I. Kim, J. Park, Y.-M. Kim, H. Shin, J. Lee, F. Caruso,Nature Nanotechnology, 2007, volume 2, pages790–795.
[12] W. L. Leong, P. S. Lee, A. Lohani, Y. M. Lam, T. Chen, S. Zhang, A. Dodabalapur, S. G. Mhaisalkar, Adv. Mater., 2008, 20: 2325-2331.
[13] S.-T. Han, Y. Zhou, Z.-X. Xu, L. -B. Huang, X. -B. Yang, V. A. L. Roy, Adv. Mater., 2012, 24: 3556-3561.
[14] E. H. Oulachgar, C. Aktik, M. Scarlete, IEEE Transactions on Electron Devices, 2010, vol. 57, no. 8, pp. 1942-1947.
[15] V. Suresh , M. S. Huang , M. P. Srinivasan and S. Krishnamoorthy , J. Mater. Chem., 2012, 22 , 21871 —21877.
[16] A. Miura, Y. Uraoka, T. Fuyuki, S. Kumagai, S. Yoshii, N. Matsukawa, I. Yamashita, Surface Science, 2007, Volume 601, Issue 15, Pages L81-L85.
[17] A. Rezk, M. H. R. Ansari, K. C. Ranjeesh, S. Gaber, D. Kumar, A. Merhi, B. R. Kaafarani, M. B. Hassine, N. E.-Atab, D. Shetty, A. Nayfeh, Sci Rep, 2023, 13, 18845.